Structural Issues in Conjugated Hydrocarbons: High-Resolution Infrared Slit-Jet Spectroscopy of *trans*-1,3-Butadiene

Marjo Halonen* and Lauri Halonen

Laboratory of Physical Chemistry, P.O. Box 55 (A.I. Virtasen aukio 1), FIN-00014 University of Helsinki, Finland; JILA, University of Colorado and National Institute of Standards and Technology, and Department of Chemistry and Biochemistry, University of Colorado, Boulder, Colorado 80309-0440

David J. Nesbitt

JILA, University of Colorado and National Institute of Standards and Technology, and Department of Chemistry and Biochemistry, University of Colorado, Boulder, Colorado 80309-0440

Received: December 4, 2003; In Final Form: January 19, 2004

First high-resolution spectroscopic and structural data for jet-cooled *trans*-1,3-butadiene have been obtained using sub-Doppler, direct absorption tunable difference frequency infrared laser methods in a pulsed slit supersonic expansion. With reduced spectral congestion at $T_{rovib} = 15$ K, high-resolution vibration−rotation spectra around 3100 cm^{-1} reveal two hybrid a/b type bands, both of which have been successfully rotationally analyzed and yield first experimental structural information on the ground state of *trans*-1,3-butadiene. The strong band $\nu_{17}(b_u)$ at 3100.63 cm^{-1} is predominantly due to "bright" state excitation of the in-phase asymmetric CH_2 stretch, with the weaker band at 3096.14 cm^{-1} probably arising from a "dark" state anharmonic mixing with ν_{17}. Furthermore, there are many local perturbations in the spectrum that can be successfully explained via anharmonic and Coriolis type coupling between ν_{17} and an additional dark state centered at 3100.65 cm^{-1}. Intensity analysis for the strong and weak bands permits a- and b-type transition moment ratios to be extracted and compared with results from electronic structure calculations.

1. Introduction

Energy stabilization due to conjugation in carbon-bonding networks is a ubiquitous phenomenon and plays an important role in a diverse variety of fields from organic chemistry to structural biology. One of the paradigmatic systems for such resonance stabilization is that of 1,3-butadiene, which represents the simplest molecule with a conjugated hydrocarbon chain. The sensitivity of these conjugation effects to rotation around the central C−C bond predicts a strong energy dependence on the torsional angle, as shown schematically in Figure 1.[1,2] There is a general consensus that the most stable energy conformer is the planar *trans*-butadiene structure, which is predicted to be the lowest in energy and thermodynamically responsible for 97% of the conformer mixture at room-temperature equilibrium. It is an asymmetric top belonging to the C_{2h} point group, but as two of the inertial moments are nearly equal it can be classified as a near-prolate symmetric rotor.

Torsional motion can convert the stable isomer, s-*trans*-butadiene, into a less stable form. There is a long standing debate over the gas-phase equilibrium geometry of this less stable minor conformer but so far no definite answer exists whether it is *cis* or *gauche*.[3−10] The s-*cis*-butadiene is planar and belongs to the point group C_{2v}. The nonplanar *gauche* conformer possesses a dihedral angle between 0° and 90° and it belongs to the C_2 point group. The *gauche* conformer is calculated to be about 10.8−14.7 kJ/mol above the *trans* form which is the lowest energy structure.[1,2] The s-*cis*-butadiene species can be regarded as an internal rotor transition state between the two nonplanar *gauche* conformers. Theoretical calculations of this *gauche*−*cis* barrier typically range from 1.6 to 4.9 kJ/mol.[1,2,7,11−14]

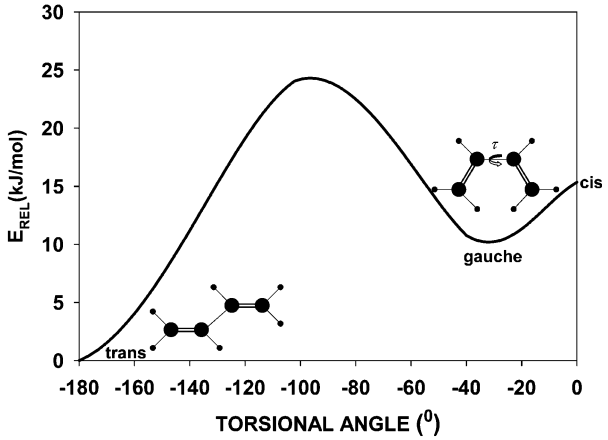

Figure 1. Potential energy curve for skeletal rotation of 1,3-butadiene around the (nominally) single C−C bond obtained using ab initio calculations.[1,2] The torsional angle τ is zero for the *cis* form but deviates from zero for the *gauche* conformer.

To the best of our knowledge, there are no high-resolution spectroscopic data on either the major or minor conformers of butadiene. The reason is clear enough for the *trans*-butadiene species, which by symmetry does not possess a permanent dipole moment and thus it is not accessible to microwave spectroscopic methods. This constraint is lifted in the infrared region, since vibrational transition intensities depend on dipole moment derivatives, which can be nonzero even in the absence of a permanent moment. However, the predicted rotational constants of butadiene are small, resulting in a dense infrared spectrum under room-temperature spectroscopic conditions. This spectral

10.1021/jp037703y CCC: $27.50
Published on Web 03/24/2004

congestion has prevented high-resolution rotational analysis in previous studies and therefore precluded determination of quantitative structural information via rotational constants on any of the butadiene conformers.

A powerful method for overcoming the spectral congestion problems described above is direct absorption laser spectroscopy in a slit supersonic expansion. This approach has the advantage of combining the long path length, to maintain high detection sensitivity under low-density conditions, with significant cooling to low rotational angular momentum quantum numbers to eliminate spectral congestion. This paper reflects ongoing efforts to exploit such high sensitivity in this high-resolution spectroscopic method to provide structural insight into different butadiene conformers. As a first step, the current work is directed toward infrared slit-jet spectroscopy and analysis of the major *trans*-butadiene conformer, in the wavenumber region corresponding to the in-phase excitation of the CH_2 asymmetric stretch.

2. Experimental Section

The experimental setup has been described in detail earlier[15,16] and therefore only the main features need to be summarized here. The source of high-resolution infrared light is from a continuous wave difference frequency laser system, whereby single mode ring dye and argon ion lasers are combined and optically subtracted in a 5 cm long temperature phase matched $LiNbO_3$ crystal, yielding ≈ 1 μW of tunable infrared power from 2400 cm^{-1} to 4500 cm^{-1}. Short term frequency noise (<1 MHz) is obtained by locking both lasers onto optical cavities. Long-term stability is maintained by locking the Ar^+ laser to an optical transfer cavity (free spectral range = 0.00833 cm^{-1}), which in turn is locked to a polarization servo loop controlled HeNe laser with a negligible frequency drift (<0.1 MHz) over several days. The optical transfer cavity also monitors transmission fringes for the tunable dye laser, therefore directly yielding stable frequency markers for calibrating the infrared difference frequency scan. Relative frequency measurements are made by interpolating marker cavity fringes and are typically precise and reproducible to 0.0001 cm^{-1}. Absolute wavenumbers are calibrated in separate experiments against well-known infrared absorbing species (e.g., $H^{35}Cl$ transitions) doped into the jet expansion.

The tunable infrared light is split into a signal and a reference beam, with the signal multipassed in a Herriot cell through a pulsed slit (40 mm $\times$ 100 μm) supersonic expansion to provide high densities, long absorption path lengths, and low jet temperatures for high-resolution measurements via direct absorption detection. The resulting signal and reference outputs from two matched InSb detectors are subtracted with fast servo loop electronics, eliminating technical "common mode" noise to the near shot noise level ($\alpha_{min} \approx 10^{-6}/Hz^{1/2}$). The expansion mixture is made from 0.8% 1,3-butadiene in excess helium diluent expanded at 400 Torr backing pressure, yielding an optical path length of 64 cm in a 16 multipass Herriott cell. The full-width at half-maximum (fwhm) optical resolution is determined from isolated spectral line widths to be $\Delta\nu \approx 50(5)$ MHz. This is already substantially sub-Doppler with respect to room-temperature absorption spectra because of collisional collimation of the expansion gases with respect to the slit axis direction, but is limited by the high helium expansion velocity and nonorthogonal crossings in the multipass cell.

3. Rotational and Vibrational Analysis

Previous room-temperature IR studies of *trans*-1,3-butadiene reveal a strong accumulation of CH stretch band intensity near 3100 cm^{-1}, which was assigned to the in-phase, asymmetric CH_2 stretch [denoted as $\nu_{17}(b_u)$]. Extraction of any structural information was prevented by intense spectral congestion and limited resolution. Under current high resolution, jet-cooled conditions, the spectra in the 3100 cm^{-1} region break into two well-defined vibrational bands, with multiple local perturbations in these bands due to resonances with combination vibrational states at the same rovibrational energy. We focus first on the two full bands, both of which arise from the *trans*-1,3-butadiene conformer, as will be shown from rotational assignment and analysis. On the basis of ab initio predictions of only one IR active "bright" state in this region [$\nu_{17}(b_u)$], this suggests the second band corresponds to a nominally "dark" state that acquires oscillator strength because of near resonant coupling with $\nu_{17}(b_u)$. Indeed, the presence of the second band (denoted herein as ν_x and approximately 4-fold down in intensity), could only be clearly recognized after significant assignment of the initial ν_{17} band was completed.

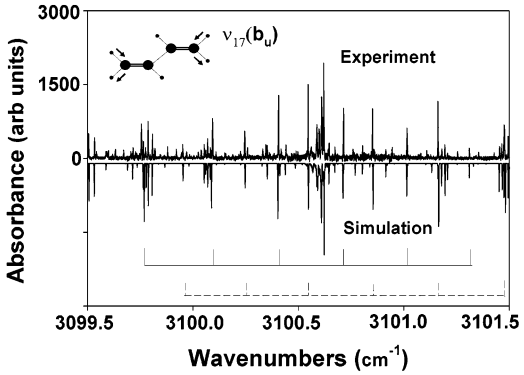

Figure 2. Part of the experimental spectrum of the a-type band origin region: $\nu_{17}(b_u)$ band of *trans*-1,3-butadiene. A simulation calculated using the appropriate parameters of Table 1 is presented below the experimental spectrum. Starting from left to right, the b-type transitions $6_{1\,6} \leftarrow 7_{0\,7}$, $5_{1\,5} \leftarrow 6_{0\,6}$,...,$1_{1\,1} \leftarrow 2_{0\,2}$ are marked with a solid line and the transitions $2_{0\,2} \leftarrow 1_{1\,1}$, $3_{0\,3} \leftarrow 2_{1\,2}$,...,$7_{0\,7} \leftarrow 6_{1\,6}$ are marked with a dashed line.

Both of the observed bands are a/b-hybrids of a near prolate asymmetric rotor, where the symbols a and b indicate that the dipole moment oscillates along the principal axes corresponding to the smallest and to the second smallest principal moments of inertia, respectively. An a-type band is characterized by $\Delta K_a = 0$ transitions and a strong central Q-branch (containing $\Delta J = 0$ transitions) and a b-type band possesses prominent $\Delta K_a = \pm 1$ transitions and several separate Q-branches. Standard spectroscopic notation is used, for example, $\Delta J = J' - J''$, where J' and J'' are upper and lower state total angular momentum quantum numbers, respectively. The label K_a refers to the near prolate symmetric top K quantum number. The stronger band $\nu_{17}(b_u)$ is mainly of b-type, but also exhibits clear a-type rotational structure near the band origin. The weaker band is also mainly b-type, though the corresponding presence of a-type structure is not as prominent as in ν_{17}. A sample spectral region illustrating P/R branch progressions and a strong central Q branch for the dominant ν_{17} vibration is shown in Figure 2. A similar representative spectral region for the 4-fold weaker ν_x band is shown in Figure 3.

Both of the observed bands have been rotationally analyzed using asymmetric rotor computer programs developed by us.[17] Assignments have been confirmed by four-line ground-state combination differences. Ground-state rotational constants can be obtained from fits to both spectra, but the ν_{17} transitions provide the most accurate set which has been used in all subsequent calculations. Altogether, 466 transition pairs with

TABLE 1: Results of the Ground and Upper State Fits of the $\nu_{17}(b_u)$ Band and of the Upper State Fit of the Unassigned, Weaker Band (ν_x) of *trans*-1,3-butadiene and of Coupled $\nu_{17}(b_u)$ and Unassigned ν_z States[a]

/cm^{-1}	ground state	$\nu_{17}(b_u)$	ν_x	$\nu_{17}(b_u)$[d]	ν_z[e]
A	1.39038820 (390)	1.3878207 (280)	1.3608774 (650)	1.3879029 (210)	1.384229 (550)
B	0.14788379 5(780)	0.14768968 (840)	0.14762939 (580)	0.14777109 (640)	0.149013 (150)
C	0.133694533 (790)	0.13358282 (500)	0.13379996 (630)	0.13350912 (530)	0.132784 (110)
ν		3100.632571 (300)	3096.143211 (250)	3100.632801 (260)	3100.65084 (410)
w_F				−0.003205 (30)	
w_C				0.003379 (110)	
δ_{fit}[b]	0.00030	0.0031	0.0016	0.0019	
Δ_v(u Å^2)[c]	−0.026	−0.093	−0.585	0.040	1.649

[a] Uncertainties in parentheses represent one-standard deviation in the least significant digit. [b] δ_{fit} is the standard deviation of the fit. [c] Δ_v is the inertial defect ($\Delta_v = I_C - I_B - I_A$). [d] $\nu_{17}(b_u)$ coupled with ν_z. [e] State perturbing $\nu_{17}(b_u)$ locally.

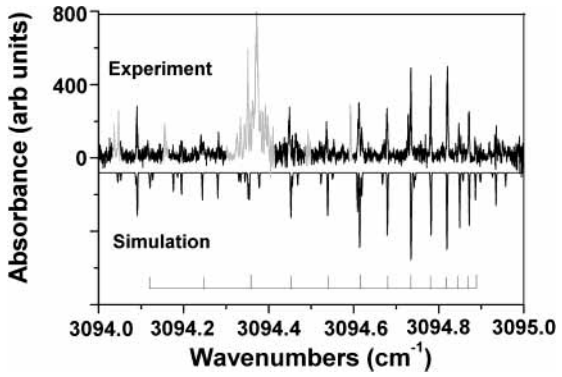

Figure 3. Sample data highlighting the presence of a second band (ν_x) associated with *trans*-1,3-butadiene in the 3100 cm^{-1} region and possibly deriving oscillator strength from IVR mixing with the allowed $\nu_{17}(b_u)$ fundamental. Peaks belonging to the stronger $\nu_{17}(b_u)$ transitions have been de-emphasized in gray to help clarify progressions from the ν_x band. A simulation calculated with least-squares fit parameters from Table 1 is presented below the experimental spectrum. Starting from left to right, the b-type transitions $13_{0\ 13} \leftarrow 13_{1\ 12}$, $12_{0\ 12} \leftarrow 12_{1\ 11}$,...,$1_{0\ 1} \leftarrow 1_{1\ 0}$ are marked with a solid line.

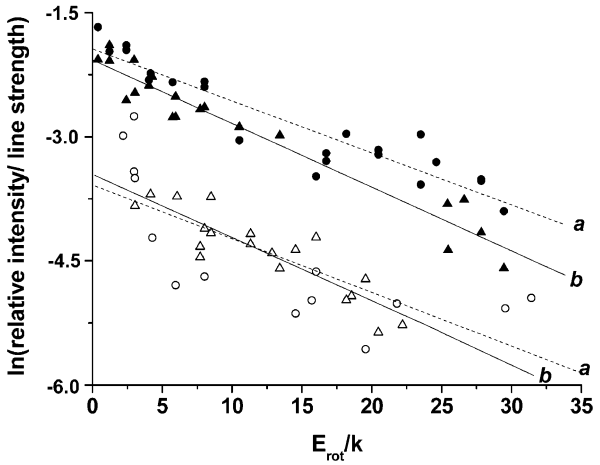

Figure 4. Boltzmann plots of experimental intensities for the $\nu_{17}(b_u)$ and the IVR induced ν_x band of *trans*-1,3-butadiene, indicating rotational temperatures of order 15 ± 3 K. The filled and open symbols ●, ▲ (○, △) refer to a-type/b-type peaks of $\nu_{17}(b_u)$ and the IVR induced ν_x band, respectively.

up to $J'' = 17$ have been included in combination difference fits for the ground state, where the rotational constants have been optimized by the nonlinear least-squares method. In the corresponding upper state fits, the ground-state rotational constants have been kept constrained and the upper state parameters (the band origin and the rotational constants) have been optimized using 275 transitions with up to $J' = 17$ for $\nu_{17}(b_u)$ and 136 transitions with up to $J' = 14$ for the weaker band. Overlapping or split peaks have been excluded. The band centers, rotational constants, and standard deviations of the fits are given in Table 1. Sample regions of simulated spectra, which indicate excellent agreement with experiment, are shown in Figures 2 and 3. Standard asymmetric rotor energy level notation $J_{K_aK_c}$ has been used where K_a and K_c are near prolate and oblate symmetric top K quantum labels, respectively. Analysis of relative intensities for a- and b-type transitions permits the transition moment ratio to be determined for both the ν_{17} band [1:0.65 (±0.05)] and ν_x band [1:0.45 (±0.1)]. A rotational temperature of 15 ± 3 K for these simulations has been determined from Boltzmann intensity plots (Figure 4), which are also consistent with previous studies of hydrocarbon species in the slit-jet expansion.[18] The intercepts of these Boltzmann plots can furthermore be used to estimate a 4:1 intensity ratio between the $\nu_{17}(b_u)$ band and the weaker ν_x band.

The observed $\nu_{17}(b_u)$ band center differs somewhat from most ab initio values,[9] although one scaled coupled-pair functional (CPF) calculation[19] predicts the band center reasonably accurately at ≈3099 cm^{-1}. The previous experimental value, 3100.5 cm^{-1}, evaluated from a medium-resolution spectrum of 1,3-butadiene, is in excellent agreement with the current results.[10] Closer inspection of standard deviations for the upper state fits to both $\nu_{17}(b_u)$ and ν_x bands (Table 1) indicates that $\nu_{17}(b_u)$ might be slightly perturbed. Inclusion of quartic centrifugal distortion terms does not improve the fit. This suggests that the perturbations are local (i.e., because of *isolated* state crossings) and cannot be simply absorbed into effective higher order rovibrational parameters. This line of analysis is pursued further in the results and discussion section.

The weaker ν_x band has a band origin roughly 4.5 cm^{-1} lower than $\nu_{17}(b_u)$. Rotational analysis clearly indicates the lower state also belonging to the *trans*-butadiene conformer, as the combination differences and rotational constants are within experimental error of the ones obtained from ν_{17} [$A_0 = 1.3904481$ (150) cm^{-1}, $B_0 = 0.14790126$ (320) cm^{-1}, and $C_0 = 0.13370145$ (260) cm^{-1} with a standard deviation of the fit 0.00042 cm^{-1}; numbers in parentheses represent 1σ]. The exact vibrational character of the ν_x band remains to be determined. The infrared inactive symmetric CH_2 stretching fundamental $\nu_1(a_g)$ is predicted to be in this same spectral region[6] and could be thought to be coupled with and acquire oscillator strength from ν_{17}. However, rovibrational resonances such as Coriolis[20] and α-resonances[21] are symmetry forbidden between ν_1 and ν_{17}; thus, ν_1 is not expected to be visible in the spectrum. Combination bands provide the most plausible explanation, which become visible via intramolecular anharmonic mixing and intensity borrowing from the nearby strong ν_{17} transition. For instance, calculated values for the $2\nu_{11} + \nu_{22}(b_u)$ and $2\nu_{15} + \nu_{22}(b_u)$ combination states [$\nu_{11}(a_u)$, $\nu_{15}(b_g)$, and $\nu_{22}(b_u)$ refer to the antisymmetric out-of-plane CH_2 bend, symmetric out-of-plane CH_2 bend, and antisymmetric CH in-plane-bend, respectively][5]

are both around 3110 cm^{-1}, on the basis of summing experimentally observed fundamental values and neglecting anharmonicity. These plausible candidates are of the correct symmetry to interact with ν_{17}. Furthermore, inclusion of anharmonic effects would tend to shift these predictions downward into better agreement with experiment. The only earlier work that mentions a weaker band is an argon matrix infrared study of 1,3-butadiene using a Knudsen cell.[5] It reports a band at 3097 cm^{-1}, but no assignment is given. The same study also gave unassigned bands at 3101 cm^{-1} and 3106 cm^{-1}.

4. Results and Discussion

The rotational constants for the upper/lower states of the different bands presented in Table 1 can be used to calculate inertial defects $\Delta_v = I_c - I_b - I_a$, where I_a, I_b, and I_c are principle moments of inertia.[22] Inertial defects contain structural information: for a planar rigid molecule, $\Delta_v \approx 0$, but can become nonzero, for example, by nonplanar conformers or excitation of the low-frequency torsional vibration. At the lowest level of structural information, the ground-state rotational constants for both bands are consistent with a planar *trans*-1,3-butadiene conformation, as can be inferred from the nearly zero value ($\Delta_v = -0.026$ u Å^2) for the inertial defect. Rotational constants can also be compared with ab initio values from CCD/6-311G++ calculations, yielding $A = 1.39123$ cm^{-1} (+0.1%), $B = 0.14689$ cm^{-1} (+0.7%), and $C = 0.13287$ cm^{-1} (+0.6%).[23] The numbers in parentheses represent fractional error, indicating excellent agreement with experiment. As expected, there are only small changes (≈0.1%) in the experimental *B*, *C* rotational constants between the ground and excited states, though there appears to be an appreciable change in *A* (≈2.2%) for the ν_x band that could signify carbon skeleton or out-of-plane bending contribution in the upper state. Both of the suggested possible assignments, $2\nu_{11} + \nu_{22}(b_u)$ and $2\nu_{15} + \nu_{22}(b_u)$, contain out-of-plane bending character because of CH_2 group excitation.

The relative intensities of the a/b-type transition moments can be used to provide additional information on the orientation of the transition moment vector in the molecular frame. The angle θ between the total transition moment vector, μ, and the *A* axis (essentially along the skeletal carbon chain) can be calculated via

$$\frac{I_b}{I_a} = \frac{|\mu_b{}^2|}{|\mu_a{}^2|} = \tan^2\theta \qquad (1)$$

For the two bands under consideration, the transition moment angles are nearly identical: $|\theta| = 57° \pm 2°$ and $66° \pm 5°$ for $\nu_{17}(b_u)$ and the combination band (ν_x), respectively. The results are somewhat smaller than the ab initio value of $\theta \approx -69°$ calculated for the $\nu_{17}(b_u)$ band using CCD 6-311G** methods,[9] though clearly close enough to remove the sign ambiguity in the experimental values. Interestingly, these ab initio estimates are also in quite good agreement with results ($\theta_{pred} \approx -70°$) from a simple bond dipole model,[8] which treats the oscillator strength as a vector sum of localized CH transition dipole moments on each of the CH_2 groups.

If one assumes that ν_x band intensity is borrowed from ν_{17}, the off-diagonal coupling constant, *w*, between ν_{17} and ν_x can be estimated from the ratio of intensities and difference in origins for the two bands. A 1:4 intensity ratio and a 4.5 cm^{-1} origin difference yield $w \approx 1.8$ cm^{-1} and deperturbed band centers separated by 2.7 cm^{-1}. This coupling coefficient and deperturbed vibrational term values can then be used as a starting point in an anharmonic resonance model with ν_{17} and ν_x states fitted simultaneously via nonlinear least-squares methods.[24] In this alternative fit of the data, the ground-state rotational constants are held fixed to the values given in Table 1, the anharmonic resonance coupling coefficient *w* is constrained to 1.8 cm^{-1}, and the transition moment for the ν_x state is kept at zero. The deperturbed band centers from such a fit are $\nu_{17}(b_u) = 3099.733103(520)$ cm^{-1} and $\nu_x = 3097.044352(830)$ cm^{-1}. The rotational constants for the $\nu_{17}(b_u)$ state are $A = 1.3946586(540)$ cm^{-1}, $B = 0.1477512(140)$ cm^{-1}, and $C = 0.1334902(100)$ cm^{-1} and those for the ν_x state are $A = 1.353382(210)$ cm^{-1}, $B = 0.1475938(200)$ cm^{-1}, and $C = 0.1338815(210)$ cm^{-1}, respectively. The standard deviation of the fit ($\delta = 0.0039$ cm^{-1}) indicates the coupled state model to be equivalent to the isolated ν_{17} band model. As expected, the mean values of both *B* and *C* rotational constants are the same within one-standard deviation when comparing the coupled and uncoupled state results.[25] Values of the *A* rotational constant are also similar, supporting the consistency of our approach. Most relevantly, the intensity predictions are in good agreement with experimentally observed band structure.

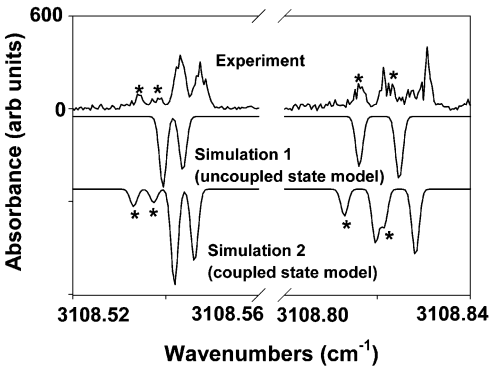

Figure 5. Sample $\nu_{17}(b_u)$ R branch spectral region [$^rR_2(5)$ and $^rR_3(6)$ transitions in symmetric top notation] and corresponding spectral predictions with ν_z perturbations included. Simulation 1 displays results for the uncoupled bright $\nu_{17}(b_u)$ state, whereas simulation 2 includes effects due to localized anharmonic resonances between bright $\nu_{17}(b_u)$ and dark ν_z states (see Table 1 for details of the fit). For both $^rR_2(5)$ and $^rR_3(6)$ transitions, asymmetry splittings as well as the additional doubling due to local resonances between ν_{17} and the ν_z perturbing state are evident (dark transitions marked with *). The two-state coupled model gives far better agreement with the observed spectra, although evidence for multiple (three-state or higher) interactions is also present in other spectral regions.

However, the standard deviations for either fitting procedure are still an order of magnitude larger than experimental uncertainty, indicating the presence of additional perturbing states. Indeed, several peaks of the ν_{17} spectrum are clearly locally perturbed and are either shifted from the calculated values or split into doublets. These perturbations occur in the upper state, as can be confirmed by identical splittings or shifts in all transitions to the same upper $J'_{K_a'K_c'}$. In contrast to the *global* anharmonic interaction discussed above, where the coupling is comparable to energy differences between unperturbed states, this is more characteristic of a *local* perturbation due to a single rovibrational dark state quickly tuning in and out of resonance with the "bright" ν_{17} state of the same total *J*. For example, all transitions to $K_a' = 1$ upper states for $J' = 7$, 8 as well as $K_a' = 3$, $J' = 5-9$ are clearly split into dark and bright state doublets. For the $K_a' = 3$ manifold, asymmetry splittings are large enough to be resolved, resulting in quartets of perturbed doublets (see Figure 5). Similarly, transitions to $J'_{0\,J'}$ in the $K_a' = 0$ upper state manifold for $J' = 8-14$ represent examples of peaks shifted systematically but not split, that is, with a perturber far enough detuned to avoid acquiring sufficient

oscillator strength to detect in the spectra. Indeed, there is occasional evidence for more than one perturber state. For example, transitions to $J'_{4\,J'-3}$ upper states in the $K_a' = 4$ manifold for $J' = 7-10$ are each split into doublets or triplets, indicating the presence of up to two perturbing states.

This behavior of small splittings and shifts over a limited range of rotational states is characteristic of weak but highly localized interactions with one or more dark states. The magnitude of these interactions and of the vibrational differences can be approximately estimated from the size of the spectral splittings, which are about 0.007−0.011 cm^{-1} in the $K_a' = 1$ and $K_a' = 3$ states. These coupling strengths and vibrational energy level differences would be more consistent with high-order combination band dark states, such as would be contributing to the total vibrational state density at these internal energies. Such high-resolution fine structure due to high-order intramolecular vibrational coupling (sometimes referred to as IVR state mixing) is well precedented, and has been extensively studied in jet-cooled CH stretch spectra by Nesbitt, Lehmann, Scoles, Perry, and others.[26−28]

In an attempt to make the analysis more quantitative, the same nonlinear least-squares program as described above has been used to analyze the small perturbations,[24] on the basis of a combination of anharmonic (Fermi resonance-type) and Coriolis-type interactions, that is, (representation I^r)

$$H_{anh}/hc = w_F + 2iw_C\hat{J}_C \qquad (2)$$

Both of these terms transform as the totally symmetric (a_g) representation and therefore can be responsible for rovibrational perturbations within vibrational states of the same symmetry. The anharmonic resonance operator mainly couples states with $\Delta K_a' = 0$ and the Coriolis-type operator states with $\Delta K_a' = \pm 1$. The data used in the calculation consist of 20 perturber transitions and 285 transitions belonging to ν_{17}. With the ground-state rotational parameters constrained to the values given in Table 1, information on the magnitude of the perturbation as well as the band centers and the rotational constants of the perturbing dark state (ν_z state in Table 1) and the ν_{17} bright state have been obtained. A localized anharmonic resonance with the ν_z state at 3100.65 cm^{-1} seems to be the explanation for many of the perturbations found in the ν_{17} band, with smaller but important effects due to the Coriolis-type term. The anharmonic term correctly reproduces the splitting in the earlier mentioned $K_a' = 1$ and the $K_a' = 3$ states where crossings with the perturber occur at $J' = 7$ and $J' = 7-8$, respectively. The Coriolis-type term is especially important for transitions to the $J'_{0\,J'}$ manifold, which exhibit significant shifts but no dark state peaks. Interestingly, the model also reproduces the $K_a' = 2$ peak positions quite well, where no splittings are observed. From the analysis, however, it turns out that these upper states are indeed also perturbed; the effects are simply much weaker because of larger separation of locally interacting states. We have tested this model further by spectral intensity calculations assuming zero transition moment for the perturber; the coupled state model reproduces experimentally observed intensities and splittings reasonably well, as demonstrated for a representative spectral region in Figure 5.

Of potential interest, the rotational constants obtained for the perturber ν_z are significantly different from the values determined for ν_{17}. Specifically, the inertial defect calculated for the perturber is 1.649 u $Å^2$ indicating the possibility that this dark vibrational state exhibits significant out-of-plane bending character. This would be consistent, for example, with a nearly resonant combination band dark state with one or multiple quanta in the torsional bending mode. This is plausible, as excitation in this lowest energy bending mode contributes predominantly to the density of combination band states in the 3100 cm^{-1} region. However, one must bear in mind that the proposed combination of anharmonic and Coriolis resonance-type effects does not predict all of the shifted or split peaks to within experimental precision, as can be seen by closer inspection of Figure 5. In addition, there are not enough data to analyze the additional perturbing states that, for example, cause multiple splittings of the $K_a' = 4$ manifold. In summary, this perturbation treatment identifies only one of presumably several states present and therefore should be considered as preliminary analysis of the major contributors.

5. Summary and Conclusions

High-resolution data on jet-cooled 1,3-butadiene in the 3100 cm^{-1} infrared region have been obtained and rotationally analyzed, permitting a first access to quantitative structural information on this species. Accurate ground vibrational state rotational constants are presented for *trans*-1,3-butadiene. These confirm a near planar geometry for the most stable conformer. At high resolution, several vibrational states are spectroscopically present in this 3100 cm^{-1} region. The strongest is the in-phase, antisymmetric CH_2 stretch fundamental (ν_{17}), which exhibits a hybrid a/b type band. This permits the transition dipole moment angle to be determined in the molecular frame, which proves to be in a good agreement with ab initio calculations as well as with predictions from a simple bond dipole model. The second strongest band, about 4-fold weaker, is also observed and rotationally analyzed, which, from a multistate analysis, is consistent with a dark state possibly borrowing intensity from the ν_{17} fundamental via a global anharmonic resonance. Evidence for additional IVR state mixing in this spectral region is also observed via localized perturbations in the ν_{17} fundamental band. These lead to additional splittings or shifts from the simulated predictions over a small rotational progression. The data are consistent with a dual tier IVR mixing of upper states in *trans*-1,3-butadiene. First, there is a global anharmonic resonance with a combination band vibration (possibly because of multiple CH_2 out-of-plane and CH in-plane bending quanta) with a relatively strong 1.8 cm^{-1} coupling matrix element, yielding two distinct albeit overlapping bands. Second, there is evidence for more localized rovibrational resonances between ν_{17} and at least one other high-order combination state, with more typical anharmonic coupling matrix elements on the order of ≈0.003 cm^{-1} in magnitude causing several isolated rovibrational perturbations in the spectrum.

Acknowledgment. This work was funded by support from the U.S. National Science Foundation (D.J.N.). M. H. and L. H. thank the Academy of Finland for financial support during a sabbatical year in Boulder, as well as JILA for support from the Visiting Fellowship program for L. H. DJN would like to thank Prof. Josef Michl for providing the original stimulus for this study, as well as for many useful discussions and ab initio predictions. We also wish to thank Dr. Michal Farnik for invaluable experimental assistance with the difference frequency spectrometer.

Supporting Information Available: v', J', K_a', K_c', v'', J'', K_a'', K_c'' and ν values. This material is available free of charge via the Internet at http://pubs.acs.org.

References and Notes

(1) Gong, X.; Xiao, H. *Int. J. Quantum Chem*. **1998**, *69*, 659.
(2) Sancho-García, J. C.; Pérez-Jiménez, A. J.; Pérez-Jordá, J. M.; Moscardó, F. *Mol. Phys*. **2001**, *99*, 47.
(3) Aston, J. G.; Szasz, G.; Woolley, H. W.; Brickwedde, F. G. *J. Chem. Phys*. **1946**, *14*, 67.
(4) Lipnick, R. L.; Garbisch, E. W., Jr. *J. Am. Chem. Soc*. **1973**, *95*, 6370.
(5) Huber-Wälchli, P.; Günthard, Hs. H. *Spectrochim. Acta A* **1981**, *37*, 285.
(6) Furukawa, Y.; Takeuchi, H.; Harada, I.; Tasumi, M. *Bull. Chem. Soc. Jpn*. **1983**, *56*, 392.
(7) Wiberg, K. B.; Rosenberg, R. E. *J. Am. Chem. Soc*. **1990**, *112*, 1509.
(8) Arnold, B. R.; Balaji, V.; Downing, J. W.; Radziszewski, J. G.; Fisher, J. J.; Michl, J. *J. Am. Chem. Soc*. **1991**, *113*, 2910.
(9) Choi, C. H.; Kertesz, M.; Dobrin, S.; Michl, J. *Theor. Chem. Acc*. **1999**, *102*, 196.
(10) De Maré, G. R.; Panchenko, Y. N.; Auwera, J. V. *J. Phys. Chem. A* **1997**, *101*, 3998.
(11) Bock, C. W.; Panchenko, Y. N. *J. Mol. Struct*. **1989**, *187*, 69.
(12) Rice, J. E.; Liu, B.; Lee, T. J.; Rohlfing, C. M. *Chem. Phys. Lett*. **1989**, *161*, 277.
(13) Alberts, I. L.; Schaefer, H. F., III. *Chem. Phys. Lett*. **1989**, *161*, 375.
(14) Skaarup, S.; Boggs, J. E.; Skancke, P. N. *Tetrahedron* **1976**, *32*, 1179.
(15) Lovejoy, C. M.; Nesbitt, D. J. *J. Chem. Phys*. **1987**, *86*, 3151.
(16) Riedle, E.; Ashworth, S. H.; Farrell, J. T., Jr.; Nesbitt, D. J. *Rev. Sci. Instrum*. **1994**, *65*, 42.
(17) Halonen, L. O.; Deeley, C. M.; Mills, I. M.; Horneman, V.-M. *Can. J. Phys*. **1984**, *62*, 1300.
(18) Uy, D.; Davis, S.; Nesbitt, D. J. *J. Chem. Phys*. **1998**, *109*, 7793.
(19) Szalay, P. G.; Karpfen, A.; Lischka, H. *J. Chem. Phys*. **1987**, *87*, 3530.
(20) Papousek, D.; Aliev, M. R. *Molecular Vibrational/Rotational Spectra*; Academia: Prague, Czech Republic, 1982.
(21) Birss, F. W. *Mol. Phys*. **1976**, *31*, 491.
(22) Gordy, W.; Cook, R. L. *Microwave Molecular Spectra*; Interscience: New York, 1970.
(23) Michl, Josef. Private communication, 2000.
(24) Halonen, L.; Duxbury, G. *J. Chem. Phys*. **1985**, *83*, 2091.
(25) Herzberg, G. *Molecular Spectra and Molecular Structure II, Infrared and Raman Spectra*; Van Nostrand: New York, 1945.
(26) McIlroy, A.; Nesbitt, D. J. *J. Chem. Phys*. **1990**, *92*, 2229. McIlroy, A.; Nesbitt, D. J.; Kerstel, E. R. Th.; Pate, B. H.; Lehmann, K. K.; Scoles, G. *J. Chem. Phys*. **1994**, *100*, 2596.
(27) Kerstel, E. R. Th.; Lehmann, K. K.; Mentel, T. F.; Pate, B. H.; Scoles, G. *J. Phys. Chem*. **1991**, *95*, 8282. Lehmann, K. K.; Scoles, G.; Pate, B. H. *Annu. Rev. Phys. Chem*. **1994**, *45*, 241.
(28) Bethardy, G. A.; Perry, D. S. *J. Chem. Phys*. **1993**, *98*, 6651; **1993**, *99*, 9400.